Imaging of $ONOO^-$ fluctuations during drug-induced liver/kidney injury *in vitro* and *in vivo* a dicyanoisophorone-based NIR fluorescent probe with large Stokes shift

Fei Kong[b#] , Hengqing Liu[c] , Jie Huang[d], Jingcan Qin [a*]

[a] Department of Radiology, Changhai Hospital, Naval Medical University, Changhai Road 168, Shanghai 200433, China

[b] School of Chemistry and Chemical Engineering, Shanghai Jiao Tong University, Dongchuan Road 800, Shanghai 200240, China

[c] School of Life Science, Fudan University, Songhu Road 2005, Shanghai 200438 China

[d] School of Biomedical Engineering, Guangzhou Medical University, Guangzhou 511436, China

Current address: Dongchuan Road 880, Shanghai 200240, China

*Corresponding author: e-mail: qinjingcan1988@163.com (JC.Q)

1.1. Reagents and instruments

All reagents used for synthesis were obtained from Aladdin without further purification. Column chromatography was performed on silica gel (200–300 mesh). ^{1}H and ^{13}C NMR spectra were recorded in DMSO-d6 at room temperature on Bruker DRX-500 (500 MHz). Mass spectra were obtained at the Mass Spectrometry Facility at Shanghai Jiao Tong University. Fluorescence studies were carried out with F-7000 Fluorescence Spectrophotometer. UV spectrum was treated in UV-2550 ultraviolet spectrophotometer. Fluorescence imaging was conducted on microscope (Nikon Eclipse). *In vivo* imaging was carried out on PE IVIS Lumina XR III. The stock solution of the probe NNP was diluted at 1 mM in DMSO for further testing.

All spectroscopic measurements of the probe (20 μM) were performed in pH 7.4, 10 mM phosphate buffer with 10% DMSO. All the spectroscopic reactions were tested at 37 ◦C. Unless otherwise noted, for all the measurements, the excitation wavelength was 490 nm, the both excitation and emission slit widths were 5 nm. The emission spectrum was measured and scanned from 550 nm to 800 nm.

1.2. Preparation of various analytes

Reactive oxygen species were prepared as follows:

H_2O_2 and ClO−: Dilution of commercially purchased solutions to the experimental concentration (100 μM) by PBS (pH 7.4). NO: Sodium (III) nitroferricyanide dihydrate was dissolved in deoxygenated ultrapure water and stored at 4 °C to prepare NO. $^{1}O_2$ was produced by addition of ClO^- solution (100 mM, 1 mL) into H_2O_2 solution (200 mM, 1 mL). $O_2^{\cdot-}$ was generated from KO_2 (35.5 mg), which was directly added into DMSO (10 mL) at a final concentration of 50 mM. ·OH was produced by addition of

ferrous chloride (0.1 M, 1 mL) into H_2O_2 solution (1.0 M, 1 mL) through a Fenton reaction. NO_2^-: Dissolving $NaNO_2$ in ultrapure water to prepare NO_2^-. $ONOO^-$: $ONOO^-$ was synthesized by the reaction of $NaNO_2$ and H_2O_2 under concentrated hydrochloric acid condition and stored in sodium hydroxide solution, and concentration of $ONOO^-$ was determined by UV-Vis spectrophotometer (ε was 1670 M^{-1} cm^{-1} at 302 nm).

Other testing analytes were prepared from the Cysteine, Glutathione, Homocysteine, NaCl, KCl, Na_2CO_3, $NaHCO_3$, $NaNO_2$, Na_2SO_4, Na_2S, $MgCl_2$, $MgSO_4$, $CuCl_2$ in the doubly distilled water.

1.3 Determination of fluorescence quantum yield

Fluorescence quantum yield (Φ) of PNDP and Compound 1 was measured by using rhodamine B (Φf= 0.97 in ethanol) as a fluorescence standard, and referred to the following equation:

$$\Phi_u = [(A_s F_u n^2)/ (A_u F_s n_0^2)] \Phi_s.$$

Where As(the standard) and Au(the sample) are the absorbance at the excitation wavelength (A is kept between 0.01 and 0.05), Fs (the standard) and Fu(the sample) are the integrated emission band areas under the same conditions, n is the refractive index of the solvent(the sample), n_0 is the refractive index of the solvent (the standard. Φ_s is fluorescence quantum yield of the standard.

1.4. Cytotoxicity

HepG2 cells and HK-2 cells were cultured in Dulbecco's Modified Eagle Medium media (DMEM, Gibco) containing 10% fetal bovine serum (FBS, Gibco) and 100 U/mL penicillin and 100 μg/mL streptomycin (Gibco) at 37 ◦C and 5% CO_2. The HepG2 cells HK-2 cells were seeded in the 96-well plates at the density of 5×10^3

cells/well and cultured overnight. Various concentrations of PNDP were added to the wells at final concentrations of 1, 5, 10, 20, 30, 50 μM. After co-incubation for 24 h, the cell viabilities were measured using CCK-8 assays. Cells treated with PBS were used as controls.

1.5. Cell imaging

HepG2 cells and HK-2 cells were cultured in Dulbecco's Modified Eagle Medium media (DMEM, Gibco) containing 10% fetal bovine serum (FBS, Gibco) and 100 U/mL penicillin and 100 μg/mL streptomycin (Gibco) at 37 ◦C and 5% CO_2. For cell imaging assays, HepG-2 cells were pretreated with PBS, 3-morpholino pyridinimine hydrochloride (SIN-1) (100 μM, 1 h), and lipopolysaccharide (LPS) (1 μg/mL, 10 h) at 37 °C, respectively. HK-2 cells were pretreated with PBS, SIN-1 (100 μM, 1 h), and cisplatin (30 μM, 24 h) at 37 °C. After washing thrice with PBS, the cells were incubated with PNDP at 20 μM for 30 min. Cells without any treatment were used as controls. The cells were then imaged respectively by a fluorescence microscope.

1.5. In vivo imaging of DILI and DIKI in mice

All animal experiments were approved by the Changhai Hospital and complied with the Guide for the Care and Use of Laboratory Animals. Acetaminophen (APAP) induced ALI model was performed by giving the mice APAP at the dosage of 400 mg/kg *via* intraperitoneal (i.p.) injection. Cisplatin induced AKI model was performed by treating mice i.p. with cisplatin (20 mg/kg). The ALI or AKI model mice and normal mice were randomly divided into two groups. One group of mice were intravenously injected (*i.v.*) with PNDP (100 μM) at 10 mL/kg and the others were injected with equal

volume of saline. The mice of each group were imaged with PerkinElmer IVIS spectrum (Waltham, MA, USA).

1.6. Hemolysis assay

The whole blood was obtained from mice in an anticoagulation tube, and the supernatant was removed after centrifugation at 1500 rpm for 5 min. The red blood cells were resuspended in saline to a 2 % RBCs suspension. Different concentrations of PDNP were added to the above suspension and incubated at 37 °C for 1 h. Blood red cells incubated with water and saline were used as positive and negative controls, respectively. After incubation, the samples were centrifuged at 1500 rpm for 5 min, and the absorbance of the supernatant at 540 nm was measured to calculate the hemolysis ratio according to the following formula:

$$Hemolysis\ rate\% = \frac{As-An}{Ap-An} \times 100;$$

where A_s, A_n, A_p represent the absorbance of the sample group, negative group, and positive group, respectively.

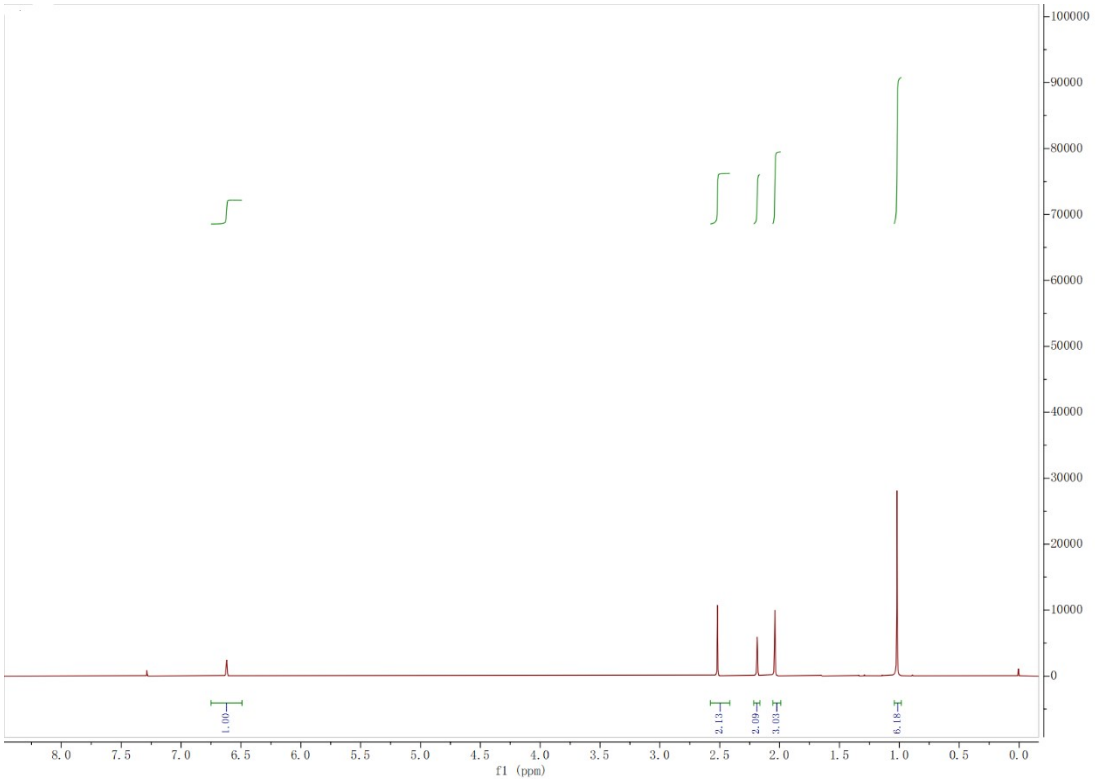

Fig. S1. ^{1}H NMR spectrum of 2-(3, 5, 5-trimethylcyclohex-2-en-1-ylidene) malononitrile

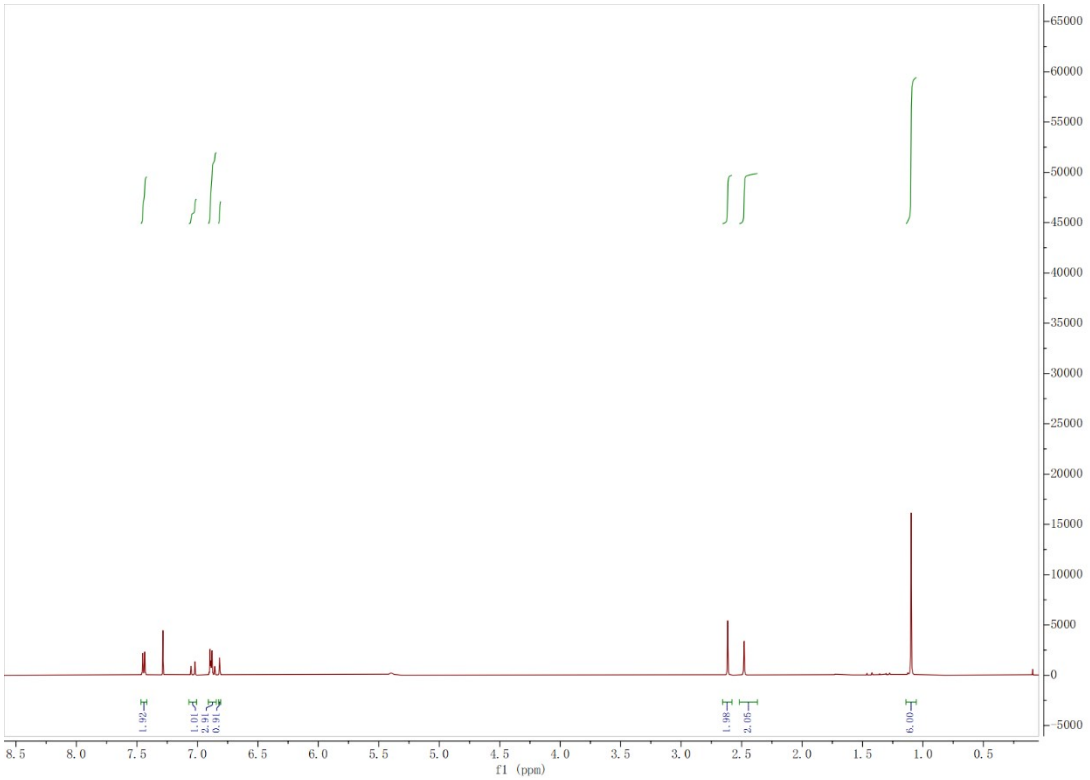

Fig. S2. ^{1}H NMR spectrum of Compound 1

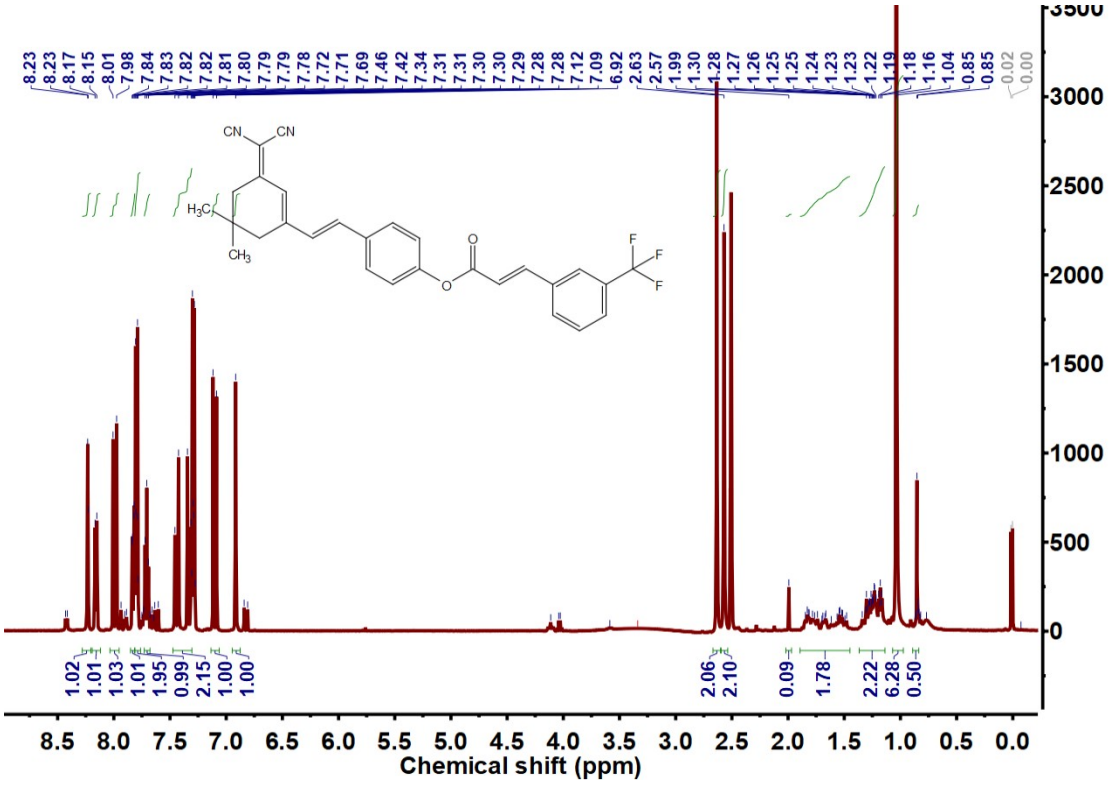

Fig. S3. ^{1}H NMR spectrum of PDNP

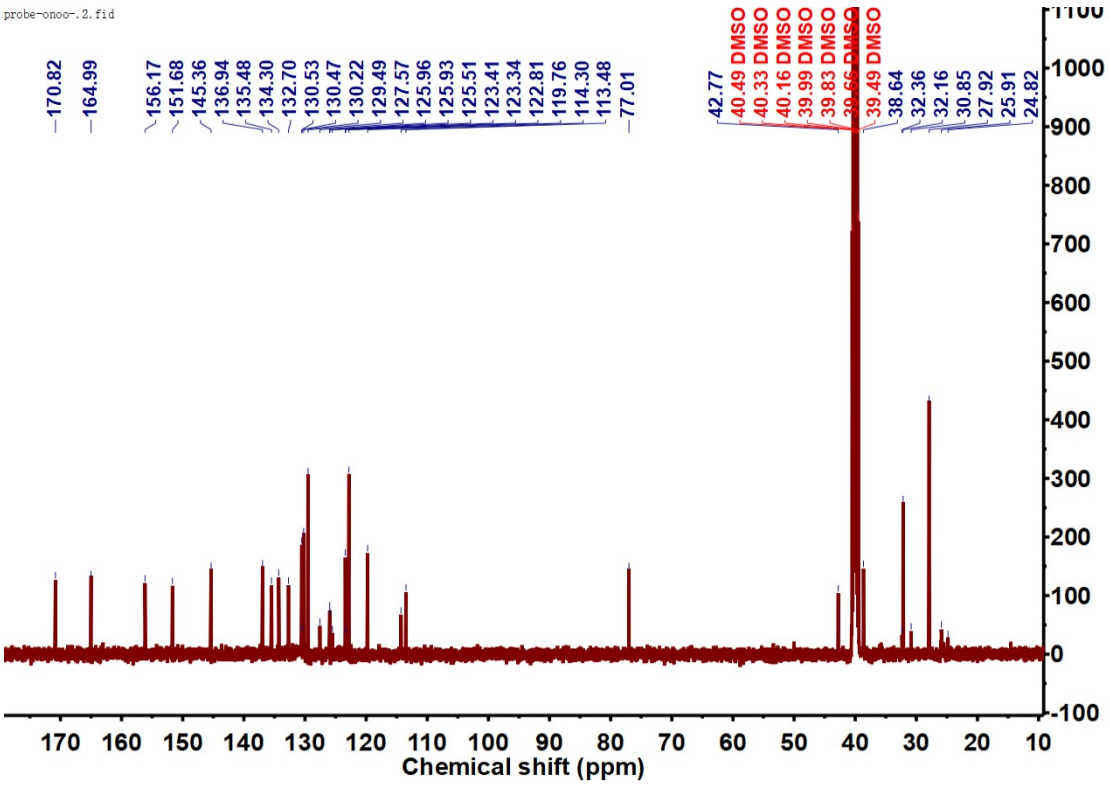

Fig. S4. ^{13}C NMR spectrum of PDNP

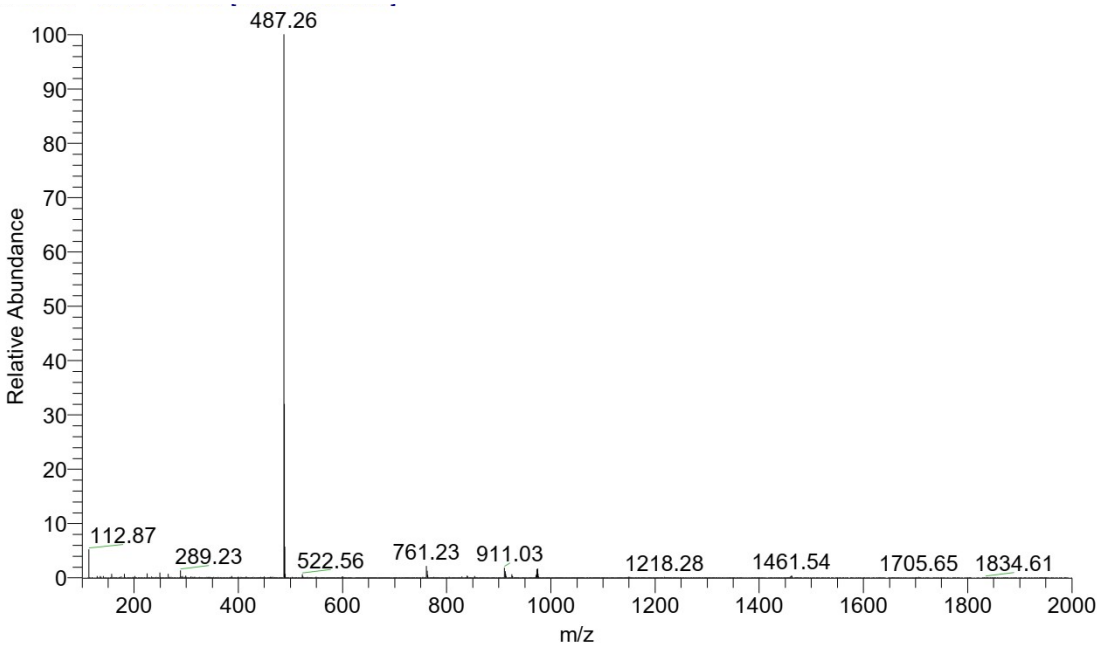

Fig. S5. The mass spectra of PDNP.

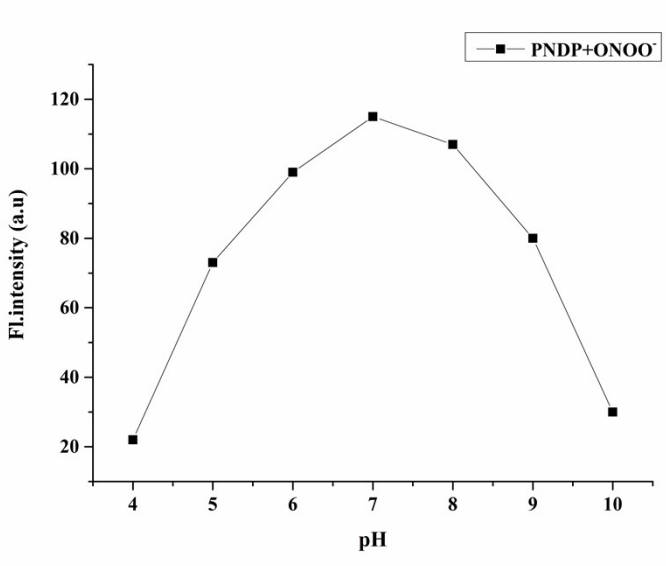

Fig. S6. Fluorescence intensity of $ONOO^-$ PNDP (20 μM) toward (100 μM) at 665 nm in different PBS buffer for 20 min. λ_{ex} = 490 nm, slit widths = 5 nm/5nm

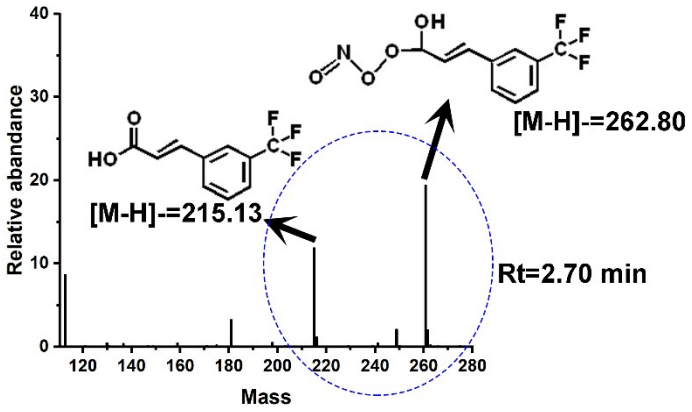

Fig. S7. The mass spectra of 3-TCA and the intermediate product formed by $ONOO^-$ and 3-TCA

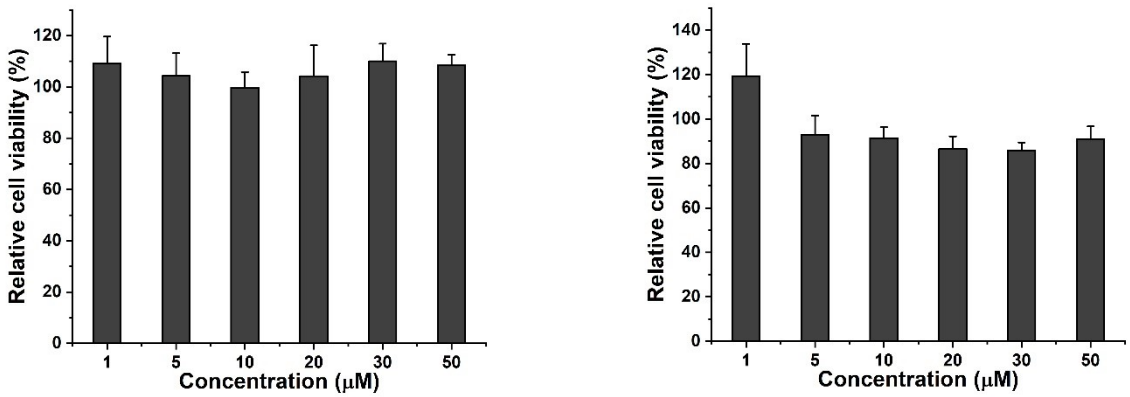

Fig. S8a.b Cytotoxicity of PDNP towards HepG2 cells(a) and HK-2 cells (b).

Fig. S9. Images of blood red cells after incubation with saline, water and various concentrations of PDNP for 1 h.

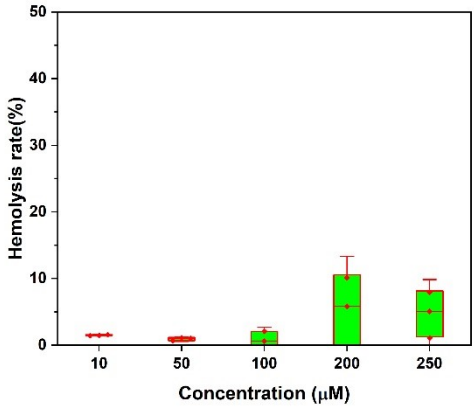

Fig. S10. Hemolysis rate of blood red cells after incubation with various concentrations of PDNP for 1 h.

Table S1. Comparison of fluorescent probes for $ONOO^-$ in recent 5 years

Probes	$\lambda_{ex}/\lambda_{em}$ (nm)	Stokes shift （nm）	LOD (nM)	Application	References

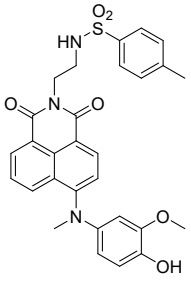	450/540	90	8.3	In vitro & in vivo Parkinson models	[1]
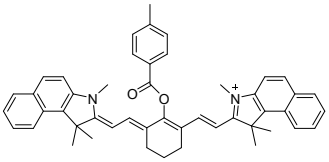	650/815	165	27.71	In vitro & in vivo acute peritonitis model	[2]
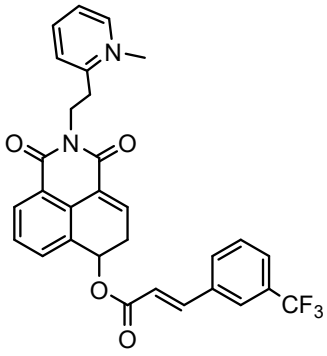	454/585	131	120	In vitro $ONOO^-$ detection	[3]
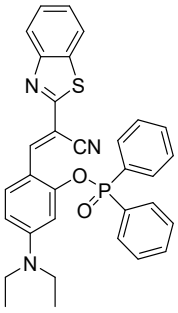	440/525	85	30	In vitro & in vivo $ONOO^-$ detection	[4]
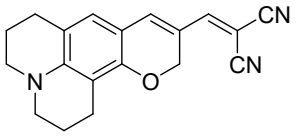	450/520	70	210	In vitro $ONOO^-$ detection	[5]

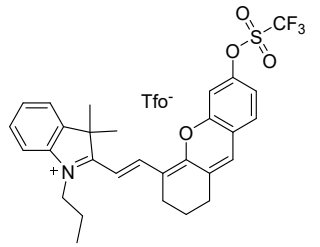	360/461	101	38.2	In vitro & in vivo DILI	[6]
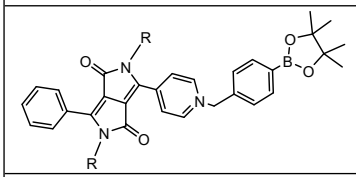	465/645	180	3.5	In vitro & in vivo DILI	[7]
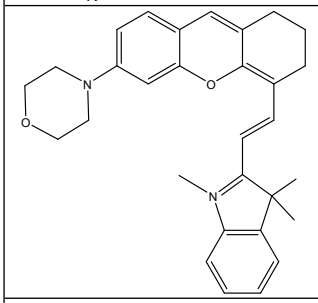	347/484 &433/583	137	120 & 77	In vitro $ONOO^-$ detection	[8]
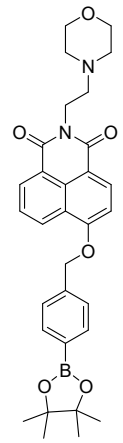	450/555	105	130	In vitro & in vivo acute liver injury	[9]
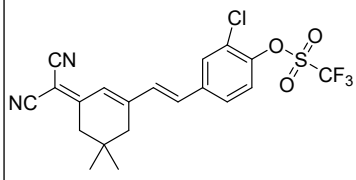	500/654	154	54.7	In vitro & in vivo acute liver injury	[10]
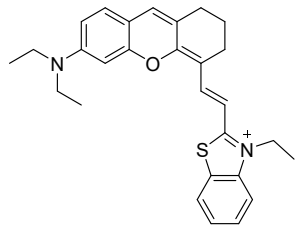	560/620 & 720/760	60	210	In vitro $ONOO^-$ detection	[11]

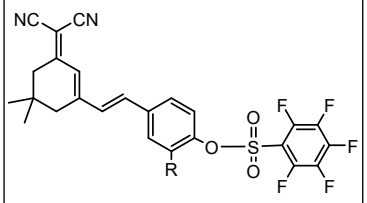	570/680	110	2.3	In vitro & in vivo lung injury models	[12]
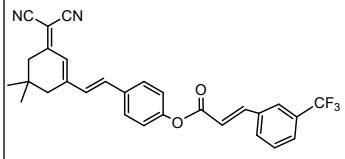	490/665	175	118.9	In vitro & in vivo DILI &DIKI models	This work

References

[1] M. Yan, H. Fang, X. Wang, J. Xu, C. Zhang, L. Xu, L. Li, A two-photon fluorescent probe for visualizing endoplasmic reticulum peroxynitrite in Parkinson's disease models, Sensors and Actuators B: Chemical 328 (2021), 129003.

[2] J. Lu, Z. Li, Q. Gao, J. Tan, Z. Sun, L. Chen, J. You, Nonoxidative Strategy for Monitoring Peroxynitrite Fluctuations in Immune Responses of Tumorigenesis, Analytical Chemistry 93(7) (2021) 3426-3435.

[3] J. Cui, S. Zang, H. Nie, T. Shen, S. Su, J. Jing, X. Zhang, An ICT-based fluorescent probe for ratiometric monitoring the fluctuations of peroxynitrite in mitochondria, Sensors and Actuators B: Chemical 328 (2021), 129069.

[4] G. Jiang, C. Li, Q. Lai, X. Liu, Q. Chen, P. Zhang, J. Wang, B.Z. Tang, An easily available ratiometric AIE probe for peroxynitrite in vitro and in vivo imaging, Sensors and Actuators B: Chemical 329 (2021), 129223.

[5] Y. Fang, R.X. Chen, H.-F. Qin, J.J. Wang, Q. Zhang, S. Chen, Y.H. Wen, K.P. Wang, Z.Q. Hu, A chromene based fluorescence probe: Accurate detection of peroxynitrite in mitochondria, not elsewhere, Sensors and Actuators B: Chemical 334 (2021), 129603.

[6] L. Wu, J. Liu, X. Tian, R.R. Groleau, S.D. Bull, P. Li, B. Tang, T.D. James, Fluorescent probe for the imaging of superoxide and peroxynitrite during drug-induced liver injury, Chemical Science 12(11) (2021) 3921-3928.

[7] N. Wang, H. Wang, J. Zhang, X. Ji, H. Su, J. Liu, J. Wang, W. Zhao, Diketopyrrolopyrrole-based sensor for over-expressed peroxynitrite in drug-induced hepatotoxicity via ratiometric fluorescence imaging, Sensors and Actuators B: Chemical 352 (2022), 130992.

[8] J. Gu, Y. Liu, J. Shen, Y. Cao, L. Zhang, Y.D. Lu, B.Z. Wang, H.L. Zhu, A three-

channel fluorescent probe for selective detection of ONOO− and its application to cell imaging, Talanta 244 (2022), 123401.
[9] K. Wang, R. Guo, X.Y. Chen, Y.S. Yang, L.Q. Qiao, M.L. Wang, Multifunctional lysosome-targetable fluorescent probe for imaging peroxynitrite in acute liver injury model, Chemical Engineering Journal 455 (2023), 140491.
[10] W. Yang, R. Liu, X. Yin, Y. Jin, L. Wang, M. Dong, K. Wu, Z. Yan, G. Fan, Z. Tang, Y. Li, H. Jiang, Peroxynitrite activated near-infrared fluorescent probe for evaluating ferroptosis-mediated acute kidney injury, Sensors and Actuators B: Chemical 393 (2023),
[11] Q. Liu, C. Dong, J. Zhang, B. Zhao, Y. Zhou, C. Fan, Z. Lu, A mitochondria-targeted ratiometric NIR fluorescent probe for simultaneously monitoring viscosity and ONOO− based on two different channels in living HepG2 cells, Dyes and Pigments 210 (2023), 111045.
[12] K. Yang, Y. Liu, M. Deng, P. Wang, D. Cheng, S. Li, L. He, Imaging peroxynitrite in endoplasmic reticulum stress and acute lung injury with a near-infrared fluorescent probe, Analytica Chimica Acta 1286 (2024),